



AFRL-SA-AR-TR-10-0345

**[Highly Sensitive Robust Damage Detection of Periodic Structures
with Piezoelectric Networking]**

**Drs. Kon-Well Wang and Jiong Tang
University of Michigan**

**AUGUST 2010
Final Report**

DISTRIBUTION A: Distribution approved for public release.

**AIR FORCE RESEARCH LABORATORY
AF OFFICE OF SCIENTIFIC RESEARCH (AFOSR)/RSA
ARLINGTON, VIRGINIA 22203
AIR FORCE MATERIEL COMMAND**

20101202161

REPORT DOCUMENTATION PAGE

The public reporting burden for this collection of information is estimated to average 1 hour per response, including the time for reviewing the data needed, and completing and reviewing the collection of information. Send comments regarding this burden estimate or any other aspect of this collection of information, including suggestions for reducing the burden, to the Department of Defense, Executive Service Directorate (0704-0188). Respondents should be aware that notwithstanding any other provision of law, no person shall be subject to any penalty for failing to comply with a collection of information if it does not display a currently valid OMB control number.

PLEASE DO NOT RETURN YOUR FORM TO THE ABOVE ORGANIZATION.

1. REPORT DATE (DD-MM-YYYY) 30-08-2010		2. REPORT TYPE Final Report		3. DATES COVERED (From - To) June 1, 2008 - May 31, 2010	
4. TITLE AND SUBTITLE Highly Sensitive and Robust Damage Detection of Periodic Structures with Piezoelectric Networking				5a. CONTRACT NUMBER	
				5b. GRANT NUMBER FA9550-08-1-0319	
				5c. PROGRAM ELEMENT NUMBER	
6. AUTHOR(S) Drs. Kon-Well Wang and Jiong Tang				5d. PROJECT NUMBER	
				5e. TASK NUMBER	
				5f. WORK UNIT NUMBER	
7. PERFORMING ORGANIZATION NAME(S) AND ADDRESS(ES) University of Michigan 2236 G.G. Brown Building 2350 Hayward Street Ann Arbor, MI 48109				8. PERFORMING ORGANIZATION REPORT NUMBER	
9. SPONSORING/MONITORING AGENCY NAME(S) AND ADDRESS(ES) Dr. David S. Stargel Program Manager, AFOSR/RSA, Air Force Office of Scientific Research 875 N. Randolph Street Suite 325, Room 3112 Arlington VA 22203-1768				10. SPONSOR/MONITOR'S ACRONYM(S) RSA	
				11. SPONSOR/MONITOR'S REPORT NUMBER(S)	
12. DISTRIBUTION/AVAILABILITY STATEMENT Approved for public release; distribution unlimited					
13. SUPPLEMENTARY NOTES					
14. ABSTRACT The goal of this research is to advance the state-of-the-art of vibration-based damage detection of bladed disks by utilizing the unique vibration localization characteristics of such periodic structures to enhance damage detection sensitivity and robustness through piezoelectric circuitry networking. In this study, we have successfully developed an innovative methodology to enhance sensitivity and robustness of vibration-based damage detection for periodic structures. A new piezoelectric network concept to temporarily increase the vibration localization in periodic structures has been established. Analytical and experimental studies have been carried out to obtain insight towards the underlying principles of the proposed approach. Fundamental understandings and design guidelines of circuitry elements that can optimize the system performance have been developed. Finally, multivariate statistical analysis tools are synthesized to evaluate and demonstrate the improvement in sensitivity and robustness of damage detection owing to the localization enhancement of the piezoelectric networking.					
15. SUBJECT TERMS structural damage identification, bladed disks, periodic structures, piezoelectric circuitry					
16. SECURITY CLASSIFICATION OF:			17. LIMITATION OF ABSTRACT	18. NUMBER OF PAGES	19a. NAME OF RESPONSIBLE PERSON
a. REPORT	b. ABSTRACT	c. THIS PAGE			Kon-Well Wang
Unclassified	Unclassified	Unclassified			19b. TELEPHONE NUMBER (Include area code) 814-777-4537

Highly Sensitive and Robust Damage Detection of Periodic Structures with Piezoelectric Networking

GRANT FA9550-08-1-0319

Final Report (June 1, 2008 to May 31, 2010)

Principal Investigators

Kon-Well Wang
Stephen P. Timoshenko Collegiate Professor of Mechanical Engineering
University of Michigan
Ann Arbor, MI 48109

Jiong Tang
Associate Professor of Mechanical Engineering
University of Connecticut
Storrs, CT 06269

Table of Contents

	<i>Page Number</i>
Table of Contents	1
Objectives	2
Summary of Efforts	2
Descriptions of Accomplishments/New Findings	2
Personnel Supported	17
Publications	17
Interactions/Transitions	17
Honors/Awards	17

Objectives

Damage detection in engine bladed disks is often performed through ultrasound and eddy current techniques that are reliable, but expensive and lack in-situ monitoring capability. Alternatively, vibration-based damage detection methods are relatively inexpensive, have real-time in-situ potential, but are generally inaccurate due to low sensitivity. The goal of this research is to advance the state-of-the-art of vibration-based damage detection of bladed disks by utilizing the unique vibration localization characteristics of such periodic structures to enhance damage detection sensitivity and robustness through piezoelectric circuitry networking.

Summary of Efforts

In this research, we have successfully developed an innovative methodology to enhance sensitivity and robustness of vibration-based damage detection for periodic structures such as engine bladed disks. A new piezoelectric network concept to temporarily increase the vibration localization in periodic structures has been established. Analytical and experimental studies have been carried out to obtain insight towards the underlying principles of the proposed approach. Fundamental understandings of vibration energy propagation/distribution in periodic systems with and without piezoelectric circuitry are reached via wave and vibration analyses. Design guidelines of circuitry elements that can optimize the system performance have been established. Finally, multivariate statistical analysis tools are synthesized to evaluate and demonstrate the improvement in sensitivity and robustness of damage detection owing to the localization enhancement of the piezoelectric networking.

Descriptions of Accomplishments and New Findings

The timely detection of damage in spatially periodic structures such as engine bladed disks is an extremely challenging task. While ultrasound and eddy current technologies have good reliability, they need significant amount of human involvement, have narrow field coverage, and are position sensitive. When applied to engine systems, they generally require the complete disassembly of engines, which leads to very long maintenance time and high cost. On the other hand, the advent of the blade-tip-timing (BTT) sensing technology is an important progress in turbomachinery bladed disk sensing. This technology uses a number of probes installed in the engine casing to sense the time instants at which the blades pass the probes. When properly analyzed, these blade passing times can lead to the vibratory amplitude information at the blade tips. There has been recent exploration in using BTT sensing for vibration response-based, online bladed disk damage detection.

While vibration-based approaches such as those using frequency-shift information to infer damage occurrence have been successfully utilized in many applications, periodic structures such as bladed disks have clustered natural frequencies, which makes it difficult to ascertain the change of these frequencies caused by damage. Another problem that is related to the detection performance is the uncertainty and variation of the structures. In particular, bladed disks, albeit manufactured with ultra-high precision, all possess certain level of manufacturing and

assembling error. The blade-to-blade random difference is often referred to as mistuning. If one uses the frequency-shift information alone, potentially fatal damage could be masked by the inherent mistuning in a bladed disk.

When the coupling between the substructures is weak in a periodic structure, it is well known that mistuning may induce the so-called vibration localization in the structure, where a single or several substructures experience excessively large vibration response. For ideally periodic structures without mistuning, the substructural coupling will split the identical substructural natural frequencies into groups of frequencies and, in any given vibration mode, all the substructures will have the same response amplitude but with certain phase difference. These frequency groups are referred to as passbands. The frequency ranges outside the passbands are the stopbands. Within a frequency stopband, wave propagation throughout the structure exhibits spatial attenuation. The width of a passband is associated with the level of coupling. In a weakly coupled situation, the passband width is small, i.e., the modal density is high. When the system has mistuning, the passband behavior is affected. Narrower passband is generally more susceptible of losing the passband characteristics due to mistuning. Essentially, in such situation, the reflected portion of the spatially propagating wave due to mistuning discontinuity between the substructures is more significant, and the successive reflections of the wave propagation lead to vibration localization for frequencies inside the original passband.

Obviously, uncontrolled vibration localization results in local concentration of vibration energy, and thus is harmful to the system durability. Nevertheless, some features of localized vibration in a periodic structure can potentially benefit damage detection. Weak coupling and high modal density make the system highly sensitive to mistuning including the damage effect. In such case, even though the natural frequency-shift caused by damage is still small and may not be noticeable when inherent mistuning is present, the vibration response patterns will be very different upon damage occurrence. In other words, for a system with strong vibration localization, even a small damage superimposed to the inherent normal mistuning in the structure may cause the vibration pattern to be significantly different from that of the healthy structure.

The overall goal of this research is to fundamentally advance the state-of-the-art of damage detection of periodic structures, by developing a highly *sensitive* and *robust* approach exploiting the unique vibration localization potential of such structures. Specifically, an innovative *piezoelectric circuitry networking methodology* that can *temporarily induce or intensify structural vibration localization to amplify the damage effect* on the system vibratory signature during the *inspection stage* is created. The network can be easily switched off (open circuit) under normal operating conditions. The overall concept is to form an electro-mechanical wave channel to enhance localization in damaged structures through energy redistribution and wave reflection. Under the temporarily intensified localization, the system response becomes extremely *sensitive* to damage occurrence (which will further enable *robust* detection), since even a small damage can now cause drastic difference in vibratory response patterns. This amplified feature change is then analyzed using a suite of robust decision making algorithms that can deal with measurement noise/uncertainty. With this new innovation, a vibration-response-based health monitoring system can become effective for periodic structures such as bladed disks, entrenching the merits of being simple and cost efficient, and can be applied to online monitoring when combined with effective sensing techniques.

During the course of this research, systematic research activities have been carried out, including experimental analysis, analytical characterization, and numerical investigation. The following steps and milestones are accomplished:

- Evaluation of the underlying principle and development of tools for integrated system synthesis;
- Creation of guidelines for network parameter design to maximize vibration localization to amplify the damage effect;
- Examination and demonstration of damage detection performance with variation and noise.

The research results and new findings are highlighted in the following sections.

Part I. Underlying principle and feasibility study

We consider a system shown in Figure 1. For illustration and without loss of generality, the periodic structure is assumed to consist of N identical cantilever beams/blades coupled with N springs. Here the springs are employed to emulate the mechanical coupling effect in generic periodic structures, such as the stiffness coupling due to disk in an engine bladed disk. To induce or enhance temporarily the vibration localization effect during inspection, identical piezoelectric inductive circuits are integrated onto all substructures/blades,

where in each circuit an inductor is connected in series with the piezoelectric transducer embedded to the substructure. These circuits are coupled through identical capacitance elements to form a global network (Figure 1b).

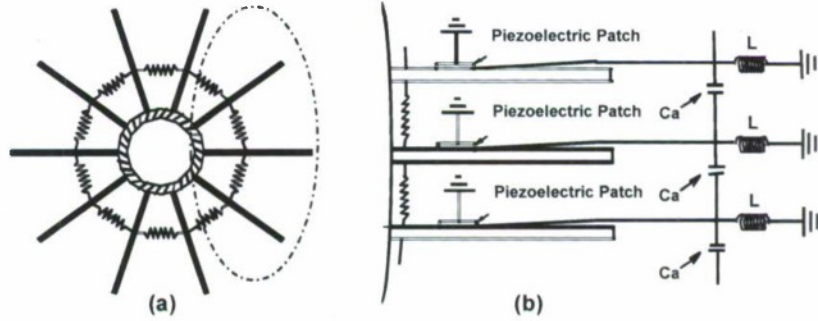


Figure 1 (a) Schematic of periodic structure; (b) Periodic structure integrated with piezoelectric network.

Our interest is in the global dynamic response of the periodic structure. While each substructure has an infinite number of degrees-of-freedom, we employ the assumed mode method to describe the substructure motion. For simple illustration, here we only use the first substructure mode for discretization. Let ϕ be the first local beam mode without the piezoelectric circuit. The transversal displacement of the j -th blade is approximated as $w_j(x,t) = \phi(x)q_j(t)$, where $q_j(t)$ is the generalized mechanical displacement ($j = 1, \dots, N$). The equations of motion of electro-mechanically integrated system can be obtained as

$$m\ddot{q}_j + g\dot{q}_j + kq_j + k_{pq}Q_j + k_c(q_j - q_{j-1}) + k_c(q_j - q_{j+1}) = f_j \quad (1a)$$

$$L\ddot{Q}_j + \frac{L}{k_a}k_{pp}(2\ddot{Q}_j - \ddot{Q}_{j-1} - \ddot{Q}_{j+1}) + \frac{L}{k_a}k_{pq}(2\dot{q}_j - \dot{q}_{j-1} - \dot{q}_{j+1}) + k_{pp}Q_j + k_{pq}q_j = 0 \quad (1b)$$

For the original mechanical structure without the piezoelectric network, the equation of motion is

$$m\ddot{q}_j + g\dot{q}_j + kq_j + k_c(q_j - q_{j-1}) + k_c(q_j - q_{j+1}) = f_j \quad (2)$$

In the above equations, m , g and k are the equivalent mass, damping and stiffness of the mechanical substructure, Q_j is the electrical charge flow in the j -th circuit, k_{pp} is the inverse capacitance of the piezoelectric transducer, k_{pq} indicates the electro-mechanical coupling, L is the circuitry inductance, and f_j is the external disturbance on the j -th blade. We define $k_a = 1/C_a$ as the inverse of the coupling capacitance. Under harmonic excitation at frequency ω , the force and displacements can be expressed as $f_j = \hat{f}_j e^{i\omega t}$, $q_j = \hat{q}_j e^{i\omega t}$ and $Q_j = \hat{Q}_j e^{i\omega t}$. Here $i = \sqrt{-1}$.

The above equations describe the perfectly periodic system without mistuning. In reality, however, there are always imperfections especially in the mechanical structure. As the common treatment in localization study, we assume that the structural mistuning only exists in the substructure stiffness. The stiffness of the j -th blade with mistuning can then be expressed as $\tilde{k}_j = k + \delta k_{mj}$, where δk_{mj} is the random stiffness mistuning with zero-mean. The damage is assumed to occur on the l -th blade only, causing stiffness loss δk_{dl} , and hence the stiffness of the l -th blade with damage is $\tilde{k}_l = k + \delta k_{dl} + \delta k_{ml}$. For non-dimensionalization, we define $\tau = \omega_m t$ where $\omega_m = \sqrt{k/m}$. The equations of motion of the system with and without the piezoelectric circuitry become, respectively,

$$-\Omega^2 x_j + 2\zeta(\Omega i)x_j + (1 + \Delta s_j)x_j + R_c^2(x_j - x_{j-1}) + R_c^2(x_j - x_{j+1}) + \xi \delta y_j = \frac{f_j}{\omega_m^2 \sqrt{m}} \quad (3a)$$

$$-\Omega^2 [y_j + R_a^2(2y_j - y_{j-1} - y_{j+1})] + \frac{\xi}{\delta} R_a^2(2x_j - x_{j-1} - x_{j+1}) + \xi \delta x_j + \delta^2 y_j = 0 \quad (3b)$$

and

$$-\Omega^2 x_j + 2\zeta(\Omega i)x_j + (1 + \Delta s_j)x_j + R_c^2(x_j - x_{j-1}) + R_c^2(x_j - x_{j+1}) = 0 \quad (4)$$

where

$$\omega_e = \sqrt{k_{pp}/L}, \quad \zeta = g/2\omega_m, \quad \delta = \omega_e/\omega_m, \quad \xi = k_{pq}/\sqrt{k_{pp}k}, \quad x_j = \sqrt{m}q_j, \quad y_j = \sqrt{L}Q_j$$

$$\Omega = \omega/\omega_m, \quad R_c = \sqrt{k_c/k}, \quad R_a = \sqrt{k_a/k_{pp}}, \quad \Delta s_j = \Delta k_{mj}/k$$

Here ω_m is the original mechanical resonant frequency of the blade, ω_e is the natural frequency of the electrical circuit ζ is the structural damping ratio, δ is essentially the inductance tuning ratio, ξ is the generalized electro-mechanical coupling coefficient which reflects the energy

transfer capability of the piezoelectric transducer, x_j and y_j are the generalized mechanical and electrical displacements, respectively, Ω is the non-dimensionalized excitation frequency; R_c is the non-dimensionalized coupling between the blades, and R_o is the coupling capacitance ratio. Δs_j is the mistuning ratio which is a zero-mean random number with stander deviation σ .

For the l -th blade with damage, the corresponding equations are

$$-\Omega^2 x_l + 2\zeta(\Omega i)x_l + (1 + \Delta s_l + \Delta k_l)x_l + R_c^2(x_l - x_{l-1}) + R_c^2(x_l - x_{l+1}) + \xi \delta y_l = \frac{f_l}{\omega_m^2 \sqrt{m}} \quad (5)$$

$$-\Omega^2 x_l + 2\zeta(\Omega i)x_l + (1 + \Delta s_l + \Delta k_l)x_l + R_c^2(x_l - x_{l-1}) + R_c^2(x_l - x_{l+1}) = 0 \quad (6)$$

where Δk_l is the stiffness loss ratio, $-1 < \Delta k_l < 0$.

The original mechanical substructures (beams/blades) all have one degree-of-freedom. With the substructural coupling, in an ideal situation without mistuning, the identical blade resonant frequencies split into a group of natural frequencies of the periodic structure. This frequency group forms a frequency passband. From the wave propagation perspective, passband is the frequency range within which the wave propagates throughout the substructures without spatial attenuation. When mistuning is present, the passband behavior is affected. When coupling is weak and the original passband is narrow, mistuning will more easily eliminate the passband characteristics and lead to more severe vibration localization. Generally, vibration localization is due to the high sensitivity of vibratory response with respect to mistuning including damage. Therefore, our underlying principle is that, if we can temporarily increase the level of vibration localization during inspection, we can highlight damage occurrence.

We have carried out experimental investigation to demonstrate this underlying principle. The overall test setup with a periodic structure emulating bladed-disk is shown in Figure 2. The structure tested is a 6-bay specimen. On each substructure, we placed piezoelectric transducers to act as exciters to emulate engine order excitation. The blades are obviously randomly mistuned. To cmulate irregularity such as damage, we added a small mass to one of the blades. The results are shown in Figure 3. We have examined cases that are weak and

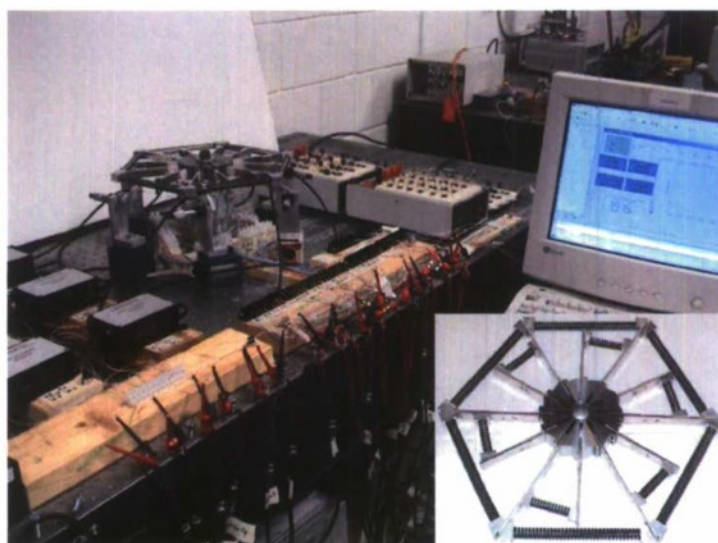


Figure 2 Experimental setup for underlying principle examination.

strong in localization to start with. For weakly localized case, there are very small differences before and after damage occurs, and the differences are generally in the noise level and are not detectable. However, for the case that we have strong localization to start with, the healthy and damaged structural responses are very different, as clearly demonstrated in Figure 3. This experiment has clearly verified our underlying principle that localization enhancement can greatly improve the vibration-based damage detection performance.

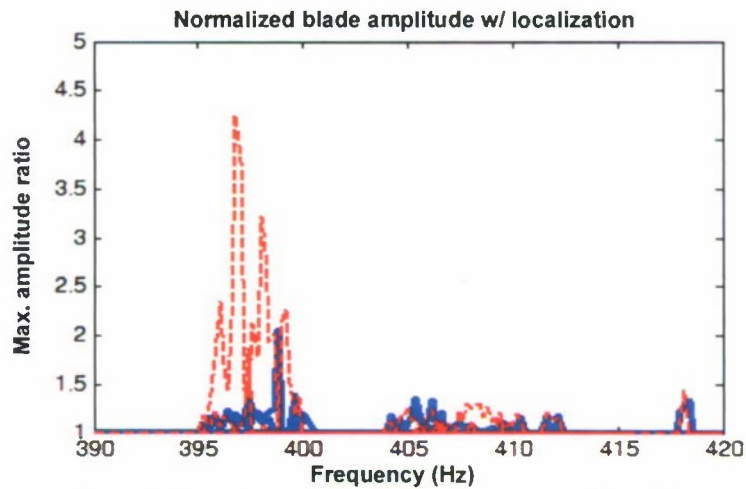


Figure 3 Experimental result of maximum normalized blade amplitude change due to damage.

Part II. Design of the piezoelectric circuitry network

In Part I of this research, we have demonstrated the underlying idea of vibration localization enhancement to benefit damage detection. For the original mechanical structure, if the mechanical coupling is not weak, the system is less sensitive to the mistuning and damage, and the vibration localization is less significant even though local wave reflection still occurs. The integration of piezoelectric inductive circuit onto the substructure adds an additional degree-of-freedom to each substructure. After these circuits are coupled through capacitance elements (Figure 1b), we obtain two frequency passbands, one corresponding to the original mechanical frequencies, and the other corresponding to the circuitry dynamics with electro-mechanical coupling. The widths and locations of these two frequency passbands are determined by a number of parameters including the circuitry elements. Our hypothesis is that, by properly designing the piezoelectric circuitry network, we can obtain a narrow frequency passband that is much more sensitive to substructural change (i.e., damage) compared to the original mechanical frequency passband. In other words, for frequencies within this narrow passband, the vibration localization will be intensified.

Wave propagation analysis and passband bandwidth

The integrated system has two wave propagation channels, one through mechanical coupling between the substructures, and the other through electrical coupling in the piezoelectric network. For each coupling type, there will be a right-going wave component and a left-going wave component. For the perfectly periodic structure, within the frequency passbands, the waves propagate freely with no spatial attenuation. The natural frequencies of the periodic structure are all inside the passbands. Outside the passbands, the propagating wave amplitude would decay exponentially. One effective way to analyze the passband feature is the wave transfer approach. For the integrated system, we define the displacement vector of the j -th interface between the adjacent subsystems as $\mathbf{u}_j = [x_{j+1} \ y_{j+1} \ x_j \ y_j]^T$, which consists of both the mechanical and

electrical generalized coordinates from the j -th and the $(j+1)$ -th subsystem. Neglecting the damping, we can re-write Equation (3) in a transfer matrix format, $\mathbf{u}_j = \mathbf{T}_j \mathbf{u}_{j-1}$, where \mathbf{T}_j is a 4×4 transfer matrix given as

$$\mathbf{T}_j = \begin{bmatrix} \frac{1 + 2R_c^2 + \Delta s_j - \Omega^2}{R_c^2} & \frac{\xi \delta}{R_c^2} & -1 & 0 \\ -\left(\frac{\xi \delta}{\Omega^2 R_a^2} + \frac{\xi}{\delta} \left(\frac{1 + \Delta s_j - \Omega^2}{R_c^2} \right) \right) & -\left(\frac{\delta^2}{\Omega^2 R_a^2} - \left(2 + \frac{1}{R_a^2} \right) + \frac{\xi^2}{R_c^2} \right) & 0 & -1 \\ 1 & 0 & 0 & 0 \\ 0 & 1 & 0 & 0 \end{bmatrix} \quad (7)$$

Obviously, the transfer matrix is a function of excitation frequency. For the mistuned system, the transfer matrix is random due to the random mistuning ratio Δs_j . For the ideally periodic system without mistuning, the transfer matrix is identical for all subsystems. For the original structure without the piezoelectric network, we have $\mathbf{v}_j = \mathbf{S}_j \mathbf{v}_{j-1}$, where $\mathbf{v}_j = [x_{j+1} \quad x_j]^T$, and the transfer matrix is given as

$$\mathbf{S}_j = \begin{bmatrix} \frac{1 + 2R_c^2 + \Delta s_j - \Omega^2}{R_c^2} & -1 \\ 1 & 0 \end{bmatrix} \quad (8)$$

Previous investigations on periodic structures have used the Lyapunov exponent to analyze the passband features and vibration localization. Mathematically, the Lyapunov exponent is obtained as

$$\gamma(\mathbf{u}_0) = \lim_{N \rightarrow \infty} \frac{1}{N} \log \|\mathbf{u}_N\| \quad (9)$$

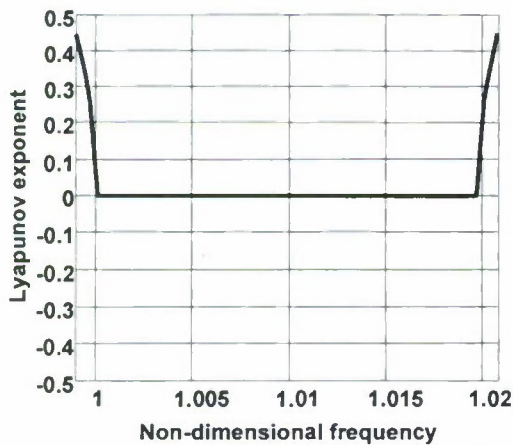


Figure 4 Lyapunov exponent of original mechanical structure without mistuning, $R_c = 0.1$.

Here \mathbf{u}_0 is the displacement vector of the first substructure, and \mathbf{u}_N is the displacement vector of the N -th substructure. The number of Lyapunov exponents is equal to twice the number of the coupling coordinates. For the original mechanical system with mechanical coupling only, there are two Lyapunov exponents which come in pair. For the integrated system analyzed in this research, there are totally four Lyapunov exponents which come

in pairs. The positive Lyapunov exponents describe the exponential decay of vibration amplitudes. Inside the passbands, the Lyapunov exponent is zero, indicating no decay. We then use the Wolf's algorithm to calculate the Lyapunov exponents of the periodic system.

We first analyze the original mechanical system without mistuning. The generalized electro-mechanical coupling coefficient is $\xi = 0.2$ and the inductance ratio is selected as $\delta = 1$ (this selection will be explained in the next section). Here we assume the structure has strong mechanical coupling, i.e., $R_c = 0.1$. As illustrated in Figure 4, there exists one frequency passband. We then analyze the system integrated with the piezoelectric network. In order to introduce weak electrical coupling into the integrated system, the capacitance value is selected as $R_a = 0.0913$, which will be further discussed in the analysis that follows. As shown in Figure 5, the integrated system with piezoelectric network has two frequency passbands, owing to the introduction of the piezoelectric network.

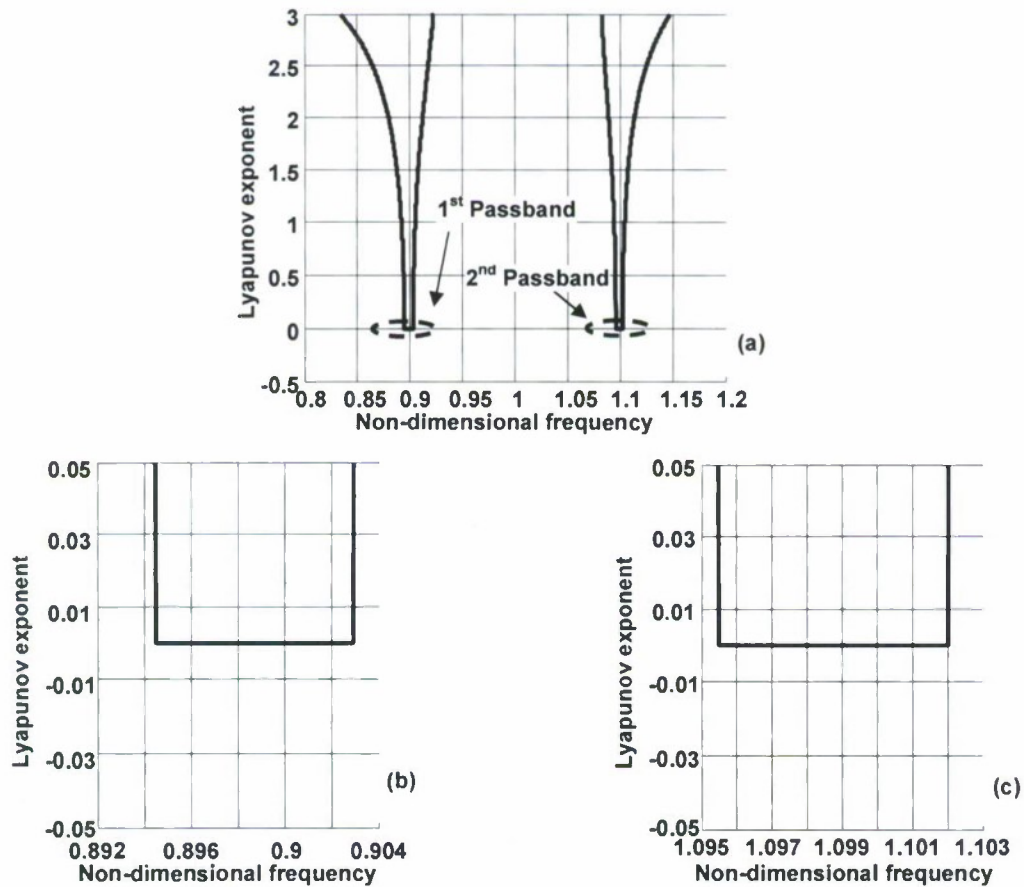


Figure 5 (a) Lyapunov exponent of system integrated with piezoelectric network, without mistuning; (b) Zoomed-in 1st passband; (c) Zoomed-in 2nd passband.

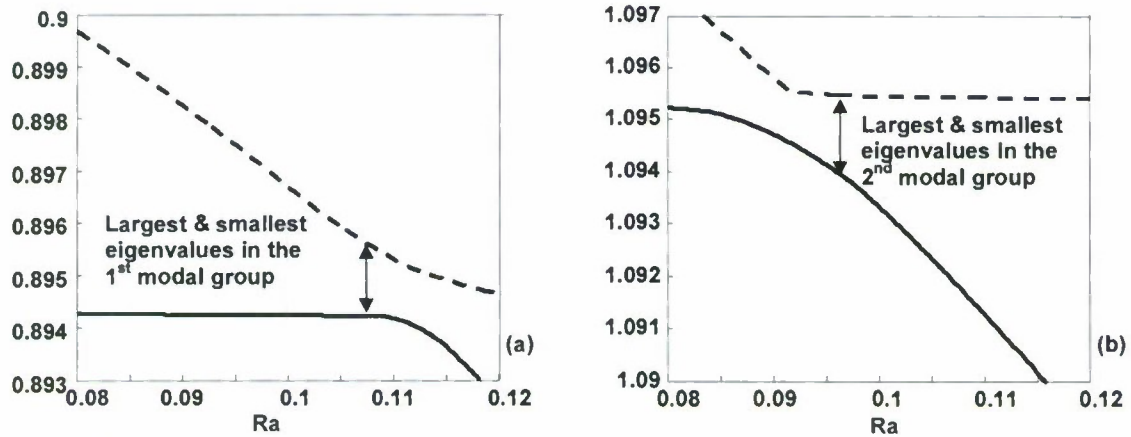


Figure 6 Eigenvalue change with different R_a ($\delta=1$) — : smallest one in the mode group; - - : largest one in the mode group. (a) 1st modal group; (b) 2nd modal group

As mentioned in Part I, the passband width generally reflects the sensitivity of the integrated system with respect to mistuning or damage occurrence. The width of the passband is closely related to the electrical elements in the piezoelectric circuitry. For tuned system without mistuning, the edges of a specific passband are determined by the smallest (marked by solid line) and the largest eigenvalues (marked by dashed line) in the corresponding modal group, plotted in Figure 6. The eigenvalues change with varying capacitance ratio R_a . We can see that: (1) for each passband, its bandwidth reaches its minimal value at certain R_a ; and (2) the minimal passband width occurs in the 2nd passband under $R_a = 0.0913$, which is referred to as the optimal value (Figure 7).

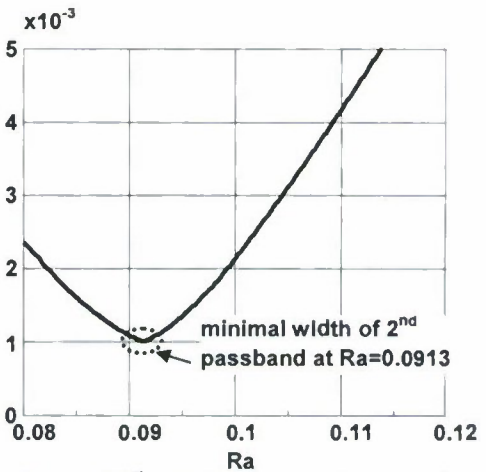


Figure 7 2nd passband width change with respect to R_a .

Inductance tuning effect and forced response magnitude

The actual damage detection will be carried out using forced responses that can be measured by the BTT measurement. The excitation form studied is the engine order excitation that is commonly used in bladed disk analysis, i.e., $f_j = \hat{f}_0 e^{i(\omega t + \phi_j)}$. Here \hat{f}_0 is the force magnitude, $\phi_j = [2\pi(E-1)(j-1)]/N$ is the phase of the force applied to the j -th blade, and E is the engine order number ($E=1, \dots, N$). For a perfectly periodic system, under a certain engine order, only the corresponding vibration mode is excited. For a mistuned system or a system with damage, however, all modes are excited even under one specific engine order, and excessive response amplitude may appear as a result of vibration localization. The frequency response of all blades will then be used in damage detection.

We now proceed to analyzing the inductance tuning effect. Recall that the non-dimensional inductance is defined as $\delta = \omega_e / \omega_m$, the ratio of the local circuit natural frequency to the uncoupled blade natural frequency. Indeed, the inductance tuning directly decides the local circuit natural frequency, and therefore dictates the dynamic coupling between the mechanical structure and the piezoelectric network. The forced-response plot of a representative blade (the 5th blade) when we select $\delta = 0.5$ is shown in Figure 8a. In this case, the first resonance is mainly related to the piezoelectric circuitry dynamics and is away from the mechanically dominant resonance. Here we can see that this additional resonance due to circuitry is 20 dB lower than the mechanically dominant resonance. When we select $\delta = 1.5$, the second resonance is mainly related to the piezoelectric circuitry dynamics and is away from the mechanically dominant resonance. Again, the additional resonance due to circuitry is 20 dB lower than the mechanically dominant resonance (Figure 8b). When we select $\delta = 1$, as the local circuit has the same natural frequency as the uncoupled blade natural frequency, the two resonant peaks have similar response magnitudes, as shown in Figure 8c. Therefore, we conclude that the strong dynamic coupling at $\delta = 1$ ensures that the additional resonant responses due to circuitry can be realistically measured, which is used as the optimal inductance tuning throughout this research.

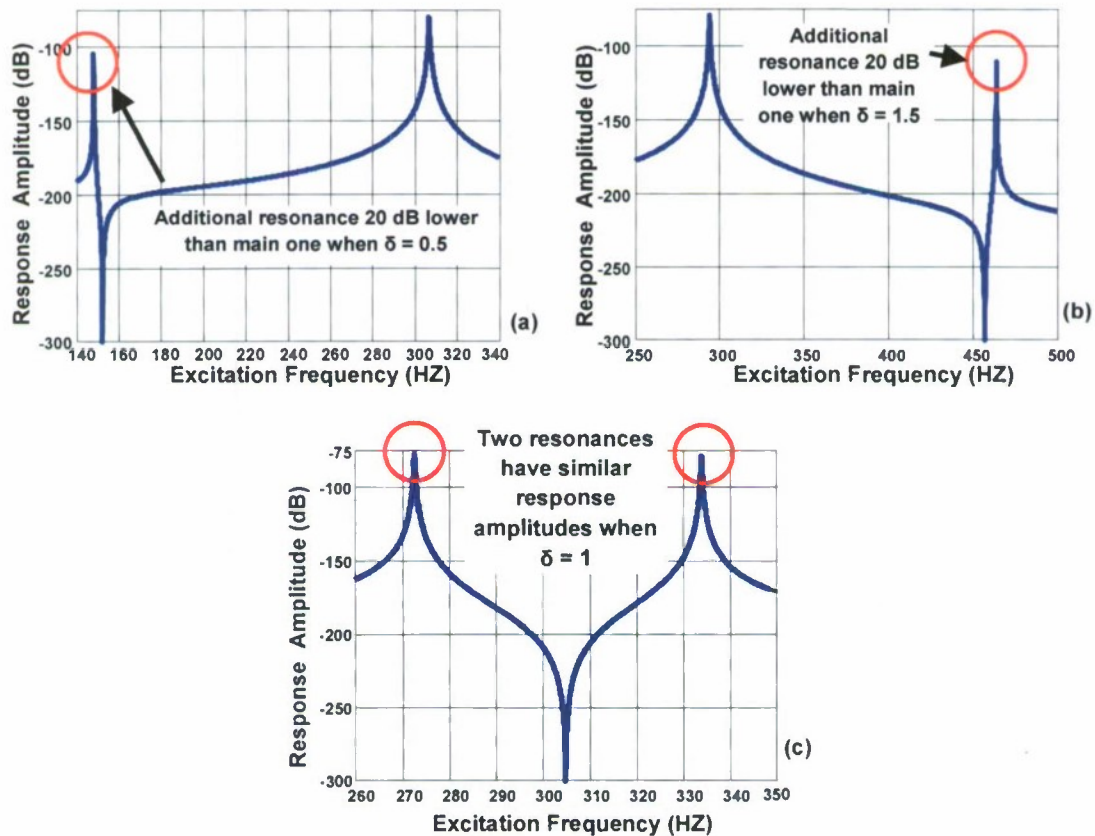


Figure 8 Resonant peak amplitude comparison under different inductance tunings. (a) $\delta=0.5$; (b) $\delta=1.5$; (c) $\delta=1$.

Localization enhancement with proper capacitance tuning

The preceding analyses on passband width and response measurements are carried out under the condition that the system is ideally periodic without mistuning or damage. We now investigate the effect of mistuning including damage under the optimal inductance and capacitance tunings (i.e., $\delta = 1$ and $R_a = 0.0913$). Figure 9b plots the Lyapunov exponents of the nearly periodic structure (with mistuning standard deviation $\sigma = 0.001$) with different coupling capacitance ratio R_a within the original frequency passband. For comparison purpose, the Lyapunov exponents of the ideally periodic structure are plotted in Figure 9a. The non-zero Lyapunov exponents indicate that the corresponding wave propagation will have amplitude decay, thereby causing vibration localization. Different R_a values affect the Lyapunov exponents differently. One can see that $R_a = 0.0913$ affects the Lyapunov exponent the most, leading to its largest increase, i.e., the largest spatial amplitude decay in wave propagation. This clearly demonstrate that the vibration localization can be maximized when we select $R_a = 0.0913$ that yields the minimal passband width.

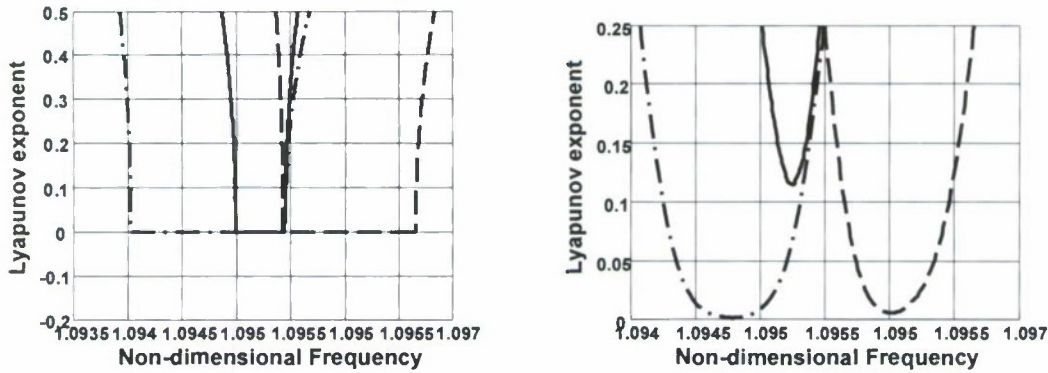


Figure 9 Lyapunov exponents at the original 2nd passband frequencies. (a) Tuned system without mistuning; (b) Mistuned system ($\sigma = 0.001$)
 - · - : $R_a = 0.085$; — : $R_a = 0.0913$ (optimal value); - - - : $R_a = 0.098$.

We further analyze the vibration modes of the systems to gain insight to vibration localization enhancement. We first consider the original mechanical structure without the piezoelectric network. For the structure with mistuning (with mistuning standard deviation $\sigma = 0.001$), the original mechanical coupling between the substructures $R_c = 0.1$ is quite large. We also assume that damage occurs on the 20th blade with stiffness loss $\Delta k_{20} = 0.2\%$. We randomly pick the 5th mode for demonstration and plot it in Figure 10. Here the dash-dot line is for the perfectly periodic structure; the dashed line is for the mistuned structure without damage, and the solid line is for the mistuned structure with damage. For the perfectly periodic structure, the mode is spatially harmonic, extended throughout the

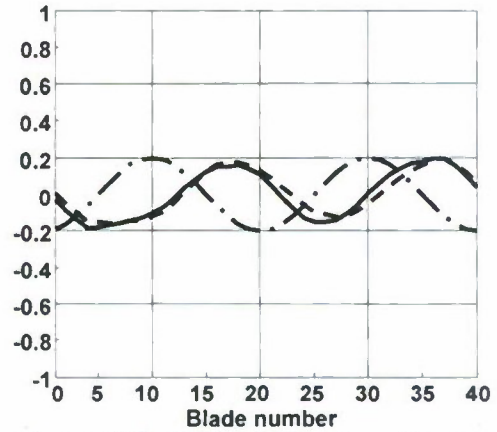


Figure 10 5th Vibration mode of mechanical structure without piezoelectric network.
 - · - : Perfectly periodic structure;
 - - - : Mistuned periodic structure;
 — : Mistuned structure with damage.

structure. When mistuning and damage occur, the mode is no longer spatially harmonic. However, since the mechanical coupling is not weak in this case ($R_c = 0.1$), the mode of the mistuned structure does not exhibit strong localization. Furthermore, no obvious pattern difference is observed after the damage occurrence.

We then analyze the system integrated with the piezoelectric network ($\delta = 1$ and $R_a = 0.0913$). As mentioned, the integrated system has two modal groups. Figure 11a shows the 5th mode for the tuned system, mistuned system and damaged system. This 5th mode belongs to the first modal group and the first passband. It is obvious that no severe localization can be observed under mistuning, and no apparent mode-shape pattern change exhibits when damage occurs. The reason is that under the tuning $\delta = 1$ and $R_a = 0.0913$, the first passband width is not minimized (Figure 6a). Figure 11b shows the 45th mode, belonging to the second modal group for the tuned, mistuned and damaged system. It is worth emphasizing that this modal group/passband reaches the minimal width under the tuning $\delta = 1$ and $R_a = 0.0913$ (Figure 6b and Figure 7). Clearly, severe vibration localization can be observed under mistuning, and the mode-shape pattern has significant change when damage occurs. These results are consistent with the preceding Lyapunov exponent analysis and wave propagation analysis, and demonstrate the effect of piezoelectric circuitry on localization enhancement. With these analyses, the optimal design of the piezoelectric circuitry has been accomplished and validated.

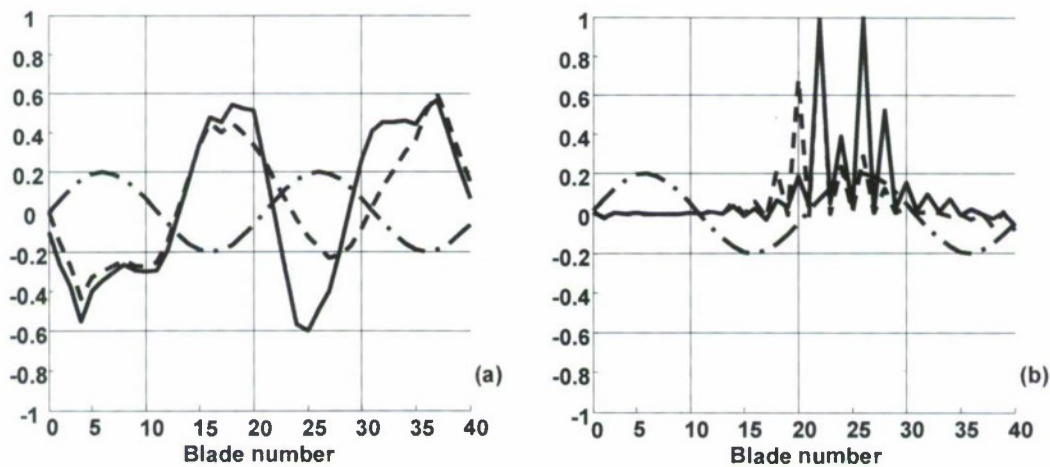


Figure 11 Vibration mode of structure integrated with piezoelectric network. (a) 5th mode from the 1st modal group; (b) 45th mode from the 2nd modal group.
 — · — : Perfectly periodic structure; - - - : Mistuned periodic structure; — : Mistuned structure with damage.

Part III. Damage detection performance investigation and robust decision making

In this part of research, we examine actual damage detection performance by using blade tip responses obtained during engine spin-up or spin-down processes, through simulated numerical investigations. For the damage detection purpose, we observe the system response within a certain frequency range. Since generally the damage effect is most significant around the resonances, we analyze the response magnitudes under frequency sweep around the resonant

frequencies. While mistuning is present in all blades, damage only occurs on one blade. In order to characterize the forced response difference, we define a performance index which is the normalized ratio of the difference between the forced responses before and after damage occurrence within certain frequency range (from ω_1 to ω_2) around the resonances. For the j -th

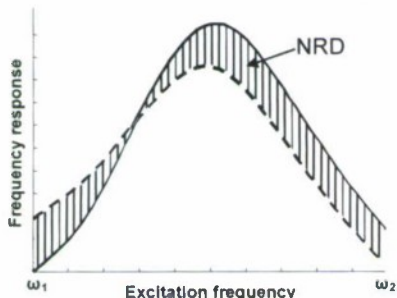


Figure 12 Damage index definition.
 — : frequency response curve of healthy baseline;
 - - : new measurement to be examined.

blade, the mathematical form of the index called “Normalized Relative Difference” (NRD) is expressed as

$$NRD_j = \int_{\omega_1}^{\omega_2} |\hat{x}_{jd} - \hat{x}_{jm}| d\omega / (\omega_2 - \omega_1) \quad (10)$$

As shown in Figure 12, the dashed line is the frequency response curve before damage, and the solid line is the one after damage; NRD_j is the shaded area between curves \hat{x}_{jm} and \hat{x}_{jd} . Clearly, the higher this index value, the more significant the change in vibration pattern (due to damage) for the j -th blade is.

Performance improvement due to localization enhancement via circuitry integration

In this illustration, we let $N = 40$, i.e., the number of blades is 40. The non-dimensionalized mechanical coupling ratio is selected as $R_c = 0.1$. The inherent mistuning ratio Δs_j has standard deviation $\sigma = 0.001$. The damping ratio is selected as $\zeta = 0.001$. Compared with the mechanical coupling ratio, the mistuning level is low, which implies that the original mechanical structure does not exhibit significant vibration localization.

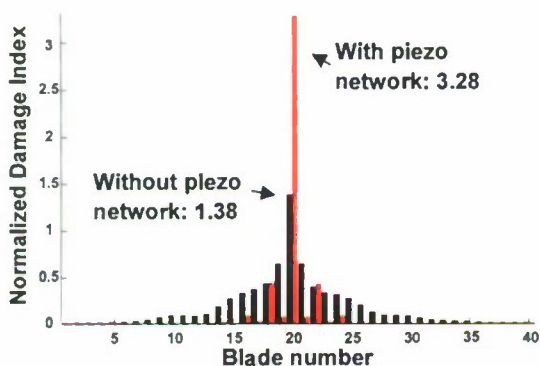


Figure 13 Normalized damage Index comparison when $k_{20}=0.1\%$
 ■ : Original structure w/o piezo network
 ■ : Integrated structure with piezo network

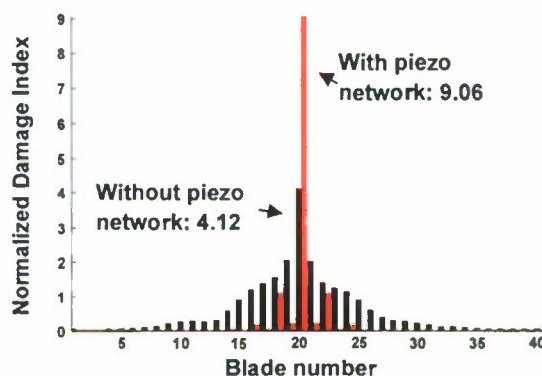


Figure 14 Normalized damage index comparison when $k_{20}=0.3\%$
 ■ : Original structure w/o piezo network
 ■ : Integrated structure with piezo network

A small damage on the 20th blade is assumed to causes stiffness loss $\Delta k_{20} = 0.1\%$. We begin our analysis with the mechanical structure without the piezoelectric circuitry, and excite the structure with the third engine order excitation to obtain the forced response of each blade. With the response curves before and after damage for the 20th blade, we can calculate the values of NRD_j ($j = 1, \dots, 40$) for all blades. The NRD_j values, plotted in Figure 13 for the mechanical

system without the piezoelectric network, are all below 1.38. The results corresponding to stiffness loss $\Delta k_{20} = 0.3\%$ are plotted in Figure 14. For this more severe damage, the NRD values for the mechanical system without the piezoelectric circuitry network are all below 4.12.

We then study the response of the bladed-disk integrated with the piezoelectric network under the aforementioned optimal circuitry tuning ($\delta = 1$ and $R_a = 0.0913$). We again analyze the forced response of each blade under the third engine order excitation with frequency sweep. The integration of the piezoelectric circuitry introduces an additional degree-of-freedom to each substructure. The integrated subsystem now has two resonances. We focus our attention on the second resonance. The reason for choosing this resonance to analyze is, as explained in Part II, this second resonance is within the passband with minimized width that has the highest modal sensitivity. We calculate NRD_j ($j = 1, \dots, 40$) for the aforementioned two damage cases and plot the results in Figure 13 and Figure 14. In both cases, with the integration of the piezoelectric network, the overall NRD values are significantly increased. The maximum is 3.28 for $\Delta k_{20} = 0.1\%$ and 9.06 for $\Delta k_{20} = 0.3\%$. The more severe the damage, the larger the difference in the NRD value is. The comparisons in Figure 13 and Figure 14 have demonstrated that the integration of piezoelectric circuitry network has more than doubled the maximum damage index.

Statistical analysis and robust decision making under variation and noise

The preceding analysis demonstrates the performance improvement under one specific set of mistuning. Since the mistuning is random in nature, we carry out Monte Carlo simulation on blade mistuning to investigate the performance from a statistical perspective. Figure 15 plots the maximum damage index under Monte Carlo simulation, when $\Delta k_{20} = 0.1\%$. The horizontal axis is the maximum damage index, and the vertical axis is the result occurrence frequency under Monte Carlo sampling. Without the piezoelectric network, the mean result of maximum damage index is 1.16, and the standard deviation is 0.09. Now with the integration of the piezoelectric network, the mean is 3.27, and the standard deviation is 0.06. Clearly, the mean of the maximum damage index mean is increased nearly three times, and the detection results have smaller standard deviation. These both indicate significant performance improvement.

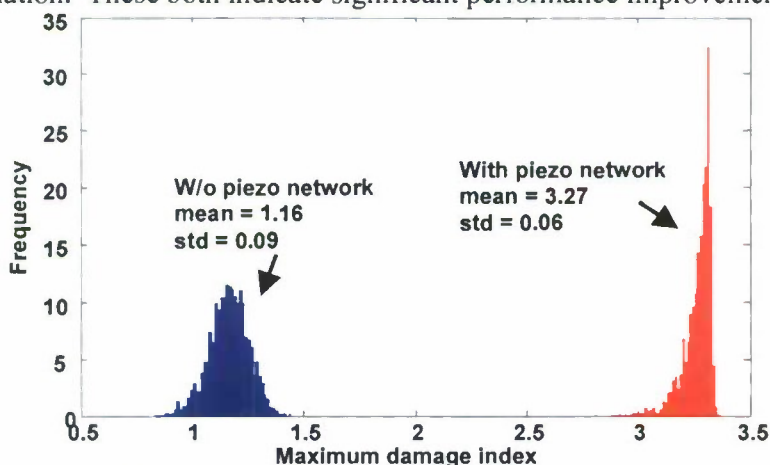


Figure 15 Monte Carlo simulation result of maximum damage index under random mistuning

In reality, the timely detection of damage is always complicated by operating uncertainty such as response measurement noise. Therefore, we have taken the measurement noise into the analysis, and synthesized a series of multivariate statistical analysis tools to achieve robust decision making. We employ the Principal Component Analysis (PCA) technique for data compression, feature extraction and de-noising. We first obtain a group of response measurement from the healthy bladed-disk system to set up the baseline. We then implement PCA, which is the eigen-analysis of variance on baseline, to separate feature space from noise effect. Once a new measurement is obtained, we can de-noise it by eigen-truncation to truncate the noise content, and calculate the damage indices. Finally, confidence-level based fault detection is facilitated by employing the Hotelling T^2 statistical analysis, which is two-step process. Firstly, we evaluate the T^2 statistics of the baseline healthy information and set up a control limit with confidence-level, e.g., 99%. In step two, we calculate the T^2 statistic of damage indices with new measurement and compare with the control limit. Damage occurrence will be declared with confidence-level if the T^2 statistics of certain damage indices exceeds the control limit specified.

Figure 16 is the result comparison under damage $\Delta k_{20} = 0.1\%$. The measurement has 1% noise with zero mean. Figure 16a is for the result without the piezoelectric network, and the T^2 statistics of all damage indices are below the control limit, which means we cannot declare damage occurrence under such noise level. Figure 16b is for the result after we integrate the piezoelectric network, and the T^2 statistics clearly exceeds the control limit, which indicates damage occurrence with 99% confidence level. Therefore, under the same noise-level, damage can be successfully detected with the integration of the piezoelectric network. This demonstrates that the new scheme can greatly increase the robustness of damage detection.

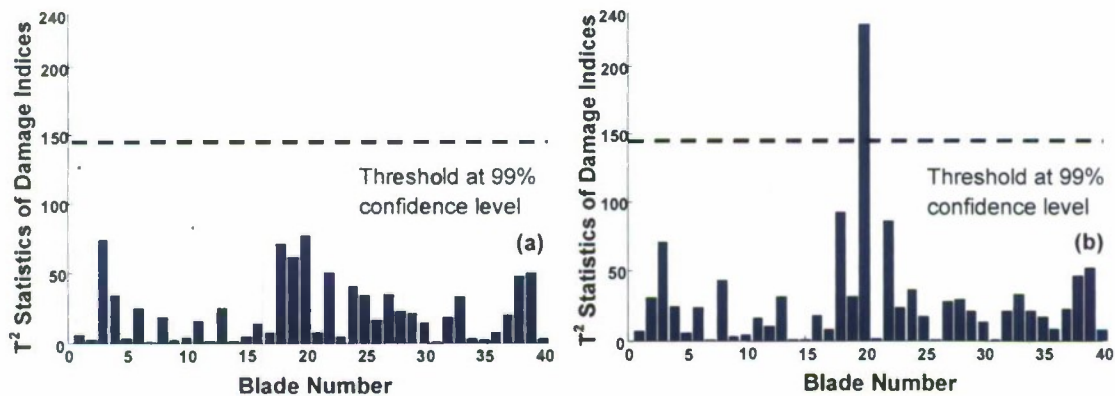


Figure 16 Robust decision making using T^2 statistical analysis (a) without piezoelectric network; (b) with piezoelectric network.

Personnel Supported

Other than the PIs, Drs. K. W. Wang and J. Tang, the project has involved two graduate students (Ryan Struzik and Ji Zhao).

Publications

Struzik, R.C., and Wang, K.W., "Intentionally mistuned piezoelectric networks for the enhancement of bladed disk structures," *Proceedings of SPIE, Smart Structures / NDE conference*, V7292, 2009.

Zhao, J., and Tang, J., "Changing dynamic behavior of periodic structure using piezoelectric circuitry," *Proceedings of SPIE, Smart Structures / NDE conference*, V7288, 2009.

Zhao, J., and Tang, J., "Anomaly amplification in dynamic response of damaged periodic structures using piezoelectric networking," *Proceedings of SPIE, Smart Structures / NDE conference*, V7643, 2010.

Zhao, J., Wang, X., and Tang, J., "Damping reduction in structures using piezoelectric circuitry with negative resistance," *Proceedings of ASME IDETC*, DETC2010-29204, 2010. Also submitted to *ASME Journal of Vibration and Acoustics*.

Zhao, J., Wang, K.W., and Tang, J., "Damage detection of periodic structures utilizing piezoelectric networking," in preparation, to be submitted to *Structural Health Monitoring*.

Interactions/Transitions

This research is directly relevant to AFOSR's mission, since the results can be applied to various Air Force systems, such as space structures, satellite antennae, and bladed-disk assemblies (e.g., fans and compressors) in gas turbine engines.

The PIs have had various interactions and technical discussions with Dr. Charles Cross and other researchers at the Wright-Patterson Air Force Research Lab (AFRL) on issues regarding fan structure implements and experimental set ups. Dr. Wang also has had communications with researchers at the Kirtland AFRL and NASA Glenn. Dr. Tang has had extensive discussions with Pratt & Whitney engineers and GE Global Research Center researchers to gather engineering insights on bladed-disk dynamics and sensing mechanisms that have greatly enhanced the level of research.

Honors/Awards

Dr. K. W. Wang is the holder of the Stephen P. Timoshenko Collegiate Chair in Mechanical Engineering at the University of Michigan. Dr. Wang is a Fellow of the American Society of

Mechanical Engineers (ASME) and a Fellow of the Institute of Physics. He is the recipient of the 2007 ASME N. O. Myklestad Award for major innovative contribution to vibration engineering and the 2008 ASME Adaptive Structures and Materials System Prize for significant contributions to the advancement of the sciences associated with adaptive structures and/or material systems. He recently also received the ASME Dynamic Systems and Controls Rudolf Kalman Best Paper Award (2009) and the ASME Adaptive Structures and Material Systems Best Paper Award in Structural Dynamics and Control (2010).